CALIBRATION OF THE CERES-MAIZE MODEL FOR LINKAGE WITH A MICROWAVE REMOTE SENSING MODEL

J. J. Casanova, J. Judge, J. W. Jones

ABSTRACT. *Stored water, i.e., soil moisture in the root zone, is the most important factor governing energy and moisture fluxes at the land surface. Crop models are typically used to estimate these fluxes and simulate crop growth and development. Remotely sensed microwave observations can be used to improve estimates of these fluxes, biomass, and yield. This research aims to calibrate a crop growth model, CERES-Maize, for a growing season of corn in north-central Florida. The CERES-Maize model was extended to weather and soil conditions of the region and calibrated using data from our second Microwave Water and Energy Balance Experiment (MicroWEX-2). The calibrated model was linked to a microwave brightness (MB) model to estimate brightness signatures of the growing corn canopy. Overall, the CERES-Maize model estimated realistic total biomass with a root mean square error (RMSE) of 1.1 Mg/ha and a Willmott d-index of 0.98. However, the partitioning of total biomass into stem and leaf biomasses were under- and overestimated, respectively. LAI matched well with the MicroWEX-2 observations with an RMSE of 0.10 and a Willmott d-index of 0.99. The model estimated realistic daily latent heat flux with an RMSE of 42 W/m^2. The soil moisture and temperature profiles of deeper soil layers matched reasonably well with observations, with RMSE of 1% to 3.5% and 1.4 to 3.7 K, respectively. Near-surface (0-5 cm) soil moisture and temperatures were less realistic because the hydrological processes near the surface need to be modeled on a much shorter timestep than is allowed by the crop model. The microwave emission model was run using observed canopy and soil inputs, as well as with the modeled canopy and soil inputs (linked crop-MB). The two methods produced similar seasonal trends in brightness temperatures with an RMS difference of 18.50 K. However, the linked model could not capture diurnal variations in brightness temperatures due to its daily timestep. Such integrated crop-MB models can be used for assimilation of remotely sensed microwave brightness in future studies to improve estimates of land surface fluxes and crop growth and development.*

Keywords. *CERES-Maize, Land surface fluxes, Microwave remote sensing, Model calibration, Soil moisture.*

Soil moisture in the vadose zone is critical in determining energy and moisture fluxes at the land surface, as well as in modeling effects of water stress on crops. Crop growth models are used to simulate soil water availability and crop development, biomass, LAI, and yield. Increasing knowledge of biophysics in the past two decades has significantly improved model parameterizations, making the crop model estimates more realistic. However, errors in model estimates can accumulate over time from unknown initial conditions, uncertain parameters, and accumulation of computational errors. One way to improve the estimations of surface fluxes such as ET, biomass, LAI, and yield is to incorporate remotely sensed data into the models. Significant research has been conducted with a variety of remotely sensed data using different strategies (Delécolle et al., 1992; Moulin et al., 1998). For example, the "forcing" strategy, in which a remotely sensed variable is substituted for the simulated one, has been used to improve soybean and corn model predictions (Doraiswamy et al., 2004). The "re-initialization/re-parameterization" strategy, in which a model is re-calibrated based on error between derived and simulated state variables, was successfully employed using optical and thermal infrared measurements from Landsat to derive LAI and water stress values for corn (Maas et al., 1989).

Data assimilation using remotely sensed soil moisture that is derived semi-empirically from microwave observations has been used to improve surface moisture and energy fluxes (Crow and Wood, 2003; Reichle et al., 2002; Burke et al., 2001; Walker and Houser, 2001; Hoeben and Troch, 2000; Lakshmi, 2000; Galantowicz et al., 2000; Houser et al., 1998; Entekhabi et al., 1994). Microwave observations at longer wavelengths ($\lambda > 3$ cm) are highly sensitive to distribution of near-surface soil moisture and temperature (Du et al., 2000; Jackson and O'Neill, 1987; Jackson, 1993). At these wavelengths, the observations are even sensitive to soil moisture beneath a vegetation canopy with a fresh biomass of up to ~6 kg/m^2 (Schmugge and Jackson, 1991). Passive observations are less affected by soil surface roughness and terrain geometry than active observations. Passive microwave remote sensing has been used to effectively estimate surface soil moisture in large-scale experiments such as the Southern Great Plains (SGP) experiments in 1997 and 1999 (Jackson et al., 1999) and the Soil Moisture Experiments (SMEX) in 2002, 2003, and 2004 (USDA-ARS, 2004). Most existing studies use variables that are derived from remotely

Submitted for review in June 2005 as manuscript number IET 5960; approved for publication by the Information & Electrical Technologies Division of ASABE in March 2006. Presented at the 2005 ASAE Annual Meeting as Paper No. 053027.

The authors are **Joaquin J. Casanova, ASABE Member,** Student, **Jasmeet Judge, ASABE Member Engineer,** Assistant Professor, and **James W. Jones, ASABE Fellow Member,** Distinguished Professor, Department of Agricultural and Biological Engineering, University of Florida, Gainesville. Florida. **Corresponding author:** Joaquin J. Casanova, Center for Remote Sensing, Department of Agricultural and Biological Engineering, University of Florida, 275 Rogers Hall, P.O. Box 110570, Gainesville, FL 32611; phone: 352-392-1864; fax: 352-392-4092; e-mail: jcasa@ufl.edu.

  ISSN 0001–2351

sensed values of either radiance (brightness) or backscatter, such as soil moisture, rather than incorporating these directly into the models. Very few studies have linked the crop models with a remote sensing model where remotely sensed measurements are used directly (Bouman, 1992; van Leeuwen and Clevers, 1994; Prevot et al., 2003). For example, Prevot et al. (2003) linked the STICS (Simulateur mulTIdisciplinaire pour les Cultures Standard) wheat model (Brisson et al., 1998) with an empirical backscattering model, CLOUD (Attema and Ulaby, 1978). The study found that assimilating active microwave data improved the crop model prediction.

Our strategy is to link a crop model to a passive microwave remote sensing model. Such integration will allow assimilation of observations of microwave brightness directly into the crop-MB model instead of assimilating semi-empirically derived soil moisture, as used in past studies. Here, we calibrate a crop growth model for a growing season of corn in north-central Florida and link the calibrated model to a physically based microwave brightness model. There are two major corn growth models, Erosion Productivity Impact Calculator (EPIC) (Williams et al., 1989) and CERES-Maize (Jones and Kiniry, 1986), that simulate hydrology, nutrient cycling, growth, and development. CERES-Maize has the advantage of being part of the well-known DSSAT Cropping System Model (DSSAT-CSM). DSSAT (Decision Support System for Agrotechnology Transfer) has been widely used for a number of years, with validated models for over 15 crops. It also allows for simulations of multi-year crop rotations (Jones et al., 2003).

In this article, we describe the field experiment conducted during a corn growing season in summer 2004. The field data were used to calibrate the CERES-Maize model. We discuss the calibration procedure and compare modeled estimates of biomass, LAI, ET, soil moisture, and temperature profiles with field observations. We describe a microwave brightness (MB) model and describe its linkage with the calibrated CERES-Maize model. We compare the brightness temperatures estimated using the integrated crop-MB model with those estimated using MB model alone with the vegetation data from the second Microwave Water and Energy Balance Experiment (MicroWEX-2).

MicroWEX-2

MicroWEX-2 was conducted from day of year (DoY) 78 (March 18) to DoY 154 (June 2) in 2004 by the Center for Remote Sensing to monitor micrometeorological, soil, and vegetation conditions as well as the microwave brightness temperatures during a growing season for sweet corn of variety Saturn SH2 (Judge et al., 2005). The experimental site (fig. 1) was a 3.6 ha (9 acre) field located at the UF/IFAS Plant Science Education and Research Unit (PSREU) in Citra, Florida. Row spacing was 76 cm, with approximately eight plants per square meter. Irrigation, fertigation, and pesticide management was conducted by the research coordinator and his team at the PSREU. The field was divided into two halves, with different fertilizer application rates; the west side of the field received a higher rate than the east side.

Data collected during MicroWEX-2 included soil moisture, temperature and heat flux, latent and sensible heat flux, wind speed and direction, upwelling and downwelling shortwave and longwave radiation, precipitation, irrigation, water table depth, and microwave brightness at 6.7 GHz (λ = 4.47 cm) every 15 min. The soil moisture, heat fluxes, and temperatures were observed at two locations in the field. Soil moisture and temperature were observed at 2, 4, 8, 16, 32, 64, and 100 cm using Campbell Scientific water content reflectometers and Vitel Hydra-probes, and thermistors and thermocouples, respectively. An Eddy covariance system measured wind speed, direction, and latent and sensible heat fluxes. A REBS CNR net radiometer measured upwelling and downwelling shortwave and longwave radiation. An Everest Interscience infrared sensor measured thermal infrared temperature. Four tipping-bucket rain gauges logged precipitation at four locations east and west of the footprint and at the east and west sides of the field. Water and fertilizer were applied through a linear-move irrigation/fertigation system. Water table depth was measured using Solinst level

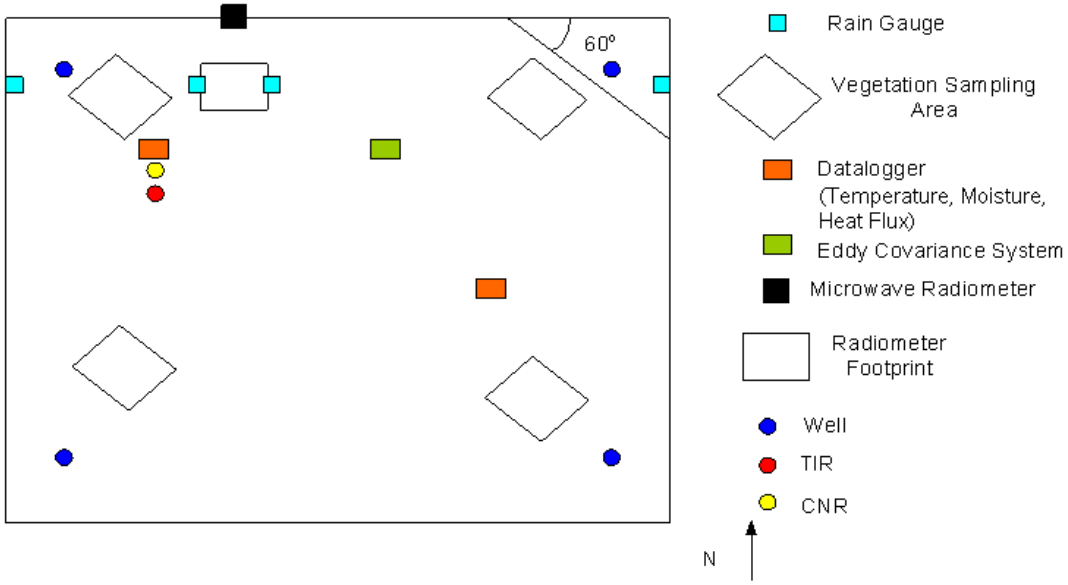

Figure 1. Field setup and instrument layout during MicroWEX-2.

loggers in a monitoring well in each quadrant. The University of Florida C-band microwave radiometer (UFCMR) measured vertically and horizontally polarized microwave emissions from a 8.54 × 8.54 m area in the northwest area of the corn field at a height of 6.0 m. Rows were at an angle of 60° from the north edge, to eliminate bias in brightness observations due to row effects.

In addition to continuously logged data, there were weekly vegetation and twice-weekly soil samplings. Vegetation sampling was conducted in four areas, one in each quadrant of the field. Samples were selected by placing a meter stick halfway between two plants and ending the sample at least 1 m from the starting point and halfway between two plants (K. Boote, personal communication, 2004). The actual row length of the sample was noted. We measured stand density, leaf number, canopy height and width, and wet and dry weights of leaves, stems, and ears. Two LAI measurements were taken in each sampling area using a Licor LAI-2000 canopy analyzer. Vegetation and soil nitrogen (as NH^+_4 and NO^-_3) were measured in each of the four sampling areas. Root length density was measured in the vadose zone at tasseling. Nitrogen was measured in each of the four wells before and after MicroWEX-2. During soil sampling, soil moisture and temperatures were observed in-row and in-furrow at depths of 2, 4, and 8 cm along eight transects at 10 to 13 locations using a Delta-T ThetaProbe soil moisture sensor and a digital thermometer to quantify the spatial variability of the field.

CERES-Maize Model

The CERES-Maize model is a part of the crop growth submodule in DSSAT-CSM. DSSAT-CSM is a modular crop simulation model with modules for soil, soil-plant-atmosphere, crop development and growth, weather, management, etc. A simulation consists of several stages: season and run initialization, rate calculation, integration, and output generation (Jones et al., 2003). For this calibration study, we focused on the performances of modules that are most significant for estimating accurate microwave signatures when linked with an MB model. These modules (soil water balance, soil temperature, soil-plant-atmosphere, and crop growth and development) estimate soil moisture and temperature, ET, biomass, LAI, and crop yield. The model determines total dry biomass using the radiation use efficiency method. Total solar radiation is partitioned into photosynthetically active radiation (PAR), and the fraction intercepted is calculated from LAI using Beer's law (Thornley and Johnson, 1990). The dry matter accumulation rate is a product of radiation use efficiency and a conversion factor. Maize growth and development is marked by eight events: germination, emergence, end of juvenile phase, floral induction (tassel initiation), 75% silking, beginning grain fill, maturity, and harvest. Transition from one developmental stage to the next is determined by the growing degree days (GDD) with a base temperature of 8°C. Vegetative growth stops on 75% silking, when reproductive growth begins in the form of grain fill. Yield is the grain fill value at harvest. Threshold GDD for each stage and grain fill parameters are contained in a cultivar file.

The CERES-Maize model determines LAI by tracking the total number of leaves and calculating a leaf area growth rate, so that the rate of increase of LAI is the product of leaf area growth and current leaf number. Leaf growth is partly determined by the number of degree days between successive leaf tip appearances, called the phyllochron interval. In addition, a leaf senescence rate is calculated based on water stress.

The soil-plant-atmosphere module estimates ET at the land surface using either the Ritchie-modified Priestley-Taylor (RPT) method (Ritchie, 1972) or the Penman-FAO (PFAO) method (Doorenbos and Pruitt, 1977). The RPT method depends only on solar radiation and temperature, while the PFAO method accounts for wind speed and relative humidity as well. Both methods first determine a total potential ET, which is partitioned into potential soil evaporation and potential plant transpiration. Potential soil evaporation is based on intercepted solar radiation reaching the soil surface as a function of temperature, wind speed, radiation, and humidity. Potential plant transpiration depends on the radiation intercepted by the canopy and temperature, wind speed, and humidity. Actual evaporation and transpiration are determined by the minimum of potential ET and the amount of available water. For soil evaporation, surface soil water is the limiting factor, while for transpiration, root water uptake is the limiting factor.

The soil is divided into ten layers, each with different constitutive properties. Soil moisture is calculated using the bucket method (Manabe, 1969). When an upper soil layer is above the drained upper limit, excess flows to the one below, in addition to computing estimates for capillary rise. Runoff is calculated using the USDA Soil Conservation Service runoff number method (USDA-SCS, 1972). Infiltration is equal to excess precipitation after runoff. Soil temperature is computed using a deep soil boundary condition and an air temperature boundary condition. The air temperature (°C) is calculated from the average of maximum and minimum daily temperatures. Soil temperature (*ST*) varies with soil layer (*L*) as (Jones et al., 2003):

$$ST(L) = T_{AVG} + \left(\frac{T_{AMP}}{2.0} \cdot COS(ALX + ZD) + DT \right) \cdot e^{ZD} \quad (1)$$

where *DT* is the difference between the average of the daily average temperatures during the previous five days and the yearly average (°C), *ZD* is depth (cm), T_{AMP} is amplitude of yearly temperature (°C), and *ALX* is the difference in days from the current day to the hottest day of the year.

Microwave Brightness Model

A microwave emission model simulates radiation emitted by the terrain (i.e., brightness temperature) at a specific wavelength (4.5 cm for our study). The brightness temperature of the terrain (T_B) is same as the physical temperature of a blackbody that would produce the observed brightness and depends on the distribution of temperature and moisture in the canopy and soil. The total brightness temperature is the sum of contributions from sky, soil, and canopy, as shown in figure 2:

$$T_B = T_{B,sky} + T_{B,soil} + T_{B,canopy} \quad (2)$$

We use the theory of radiative transfer to model T_B (Ulaby et al., 1981). This simplified model accounts for non-scattering emission from sky, vegetation, and soil as:

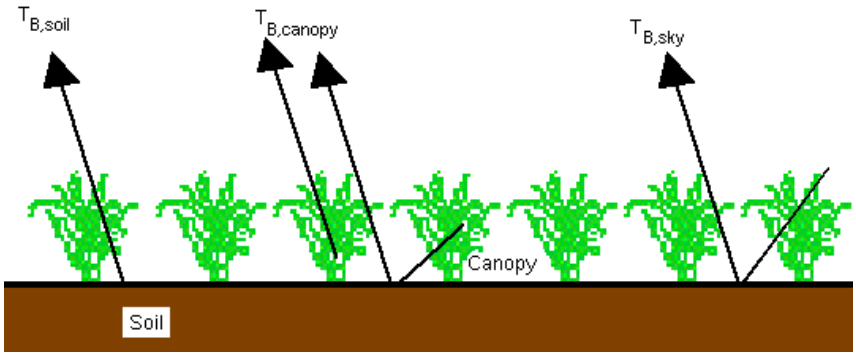

Figure 2. Radiative transfer paths and brightness contributions in the microwave emission model.

$$T_B = T_{B,sky} \cdot \Gamma \cdot e^{-2\tau} + T_{soil} \cdot (1-\Gamma) \cdot e^{-\tau}$$
$$+ T_{canopy} \cdot (1-e^{-\tau})(1+\Gamma e^{-\tau}) \quad (3)$$

where $T_{B,sky}$ is the physical temperature of the cosmic sky, Γ is soil reflectivity, τ is canopy optical depth (a measure of canopy transmissivity), T_{soil} is the effective physical temperature of the soil, and T_{canopy} is the effective physical temperature of the canopy. The model ignores atmospheric contribution as this is insignificant for studies using ground-based radiometers like ours. The first term in equation 3 accounts for sky emission transmitted through the canopy, reflected by the soil, and transmitted back through the canopy. The second term accounts for soil emission transmitted through the canopy, and the third term accounts for the upwelling canopy emission and the downwelling canopy emission reflected by the soil and transmitted through the canopy.

Optical depth (τ) is modeled as a function of vegetation water content, M_w (kg/m^2) (Schmugge and Jackson, 1991):

$$\tau = b \cdot M_w \quad (4)$$

where b is an empirical constant (0.015). Soil reflectivity is a function of the polarization-dependent refractive index (n) in the microwave region and the sensor look angle (θ), given by the Fresnel equations (Ulaby et al., 1981):

$$\Gamma_v = \left| \frac{n^2 \cos\theta - \sqrt{n^2 - \sin^2\theta}}{n^2 \cos\theta + \sqrt{n^2 - \sin^2\theta}} \right|^2 \quad (5)$$

$$\Gamma_h = \left| \frac{\cos\theta - \sqrt{n^2 - \sin^2\theta}}{\cos\theta + \sqrt{n^2 - \sin^2\theta}} \right|^2 \quad (6)$$

where the subscripts v and h indicate vertical and horizontal polarization. The refractive index of the moist soil is estimated by a dielectric mixing model (Dobson et al., 1985), which accounts for refractive indices of different soil components.

Model Calibration

The CERES-Maize model was ported to the Linux OS (G. Hoogenboom, personal communication, 2004) and calibrated using data from MicroWEX-2. This section describes the calibration procedure.

Initialization

CERES is the crop submodule for cereal crops, including maize. CERES-Maize uses three files for determining growth and development characteristics: the species file, the ecotype file, and the cultivar file. The species file contains defining characteristics of corn, including root growth parameters, seed initial conditions, nitrogen and water stress response coefficients, nitrogen uptake parameters, base and optimum temperatures for grain fill and photosynthesis, and radiation and CO_2 parameters governing photosynthesis. The ecotype file specifies thermal time development, radiation use efficiency, and light extinction coefficients for three main types of corn. The cultivar file specifies the six cultivar coefficients that describe the growth and development characteristics for different maize cultivars. These are:

- P1: degree days between emergence and end of juvenile stage.
- P2: development delay for each hour increase in photo–period past optimum photoperiod.
- P5: degree days from silking to maturity.
- G2: maximum possible number of kernels per plant.
- G3: kernel filling rate during the linear grain filling stage and under optimum conditions (mg/day).
- PHINT: phyllochron interval, i.e., the interval in thermal time (degree days) between leaf tip appearances.

Soil properties such as hydraulic conductivity and texture were taken as the default values for the soil type from DSSAT that matched closely with our field site (Millhopper fine sand). The drained lower limit of the top nine soil layers was set to the minimum soil moisture (0.05) observed during MicroWEX-2. The initial soil moisture for all the layers was set equal to 0.2. The model calibration was found to be insensitive to the choice of initial moisture conditions because an irrigation event at planting reset the soil moisture profile of sandy soil.

Inputs

Most of the inputs for the model calibration were obtained from the MicroWEX-2 dataset. These included daily incoming solar radiation, precipitation, irrigation, fertigation, and wind speed. Maximum and minimum daily temperature and relative humidity were obtained from the micrometeorological dataset collected for the Agricultural Field-Scale Irrigation Requirement Simulation (AFSIRS) study at a nearby site at the PSREU (M. Dukes, personal communication, 2004).

Table 1. Cultivar coefficient values in the calibrated CERES-Maize model.

Cultivar Coefficient	Value
P1	157.20
P2	1.000
P5	811.20
G1	853.00
G3	10.4
PHINT	40.33

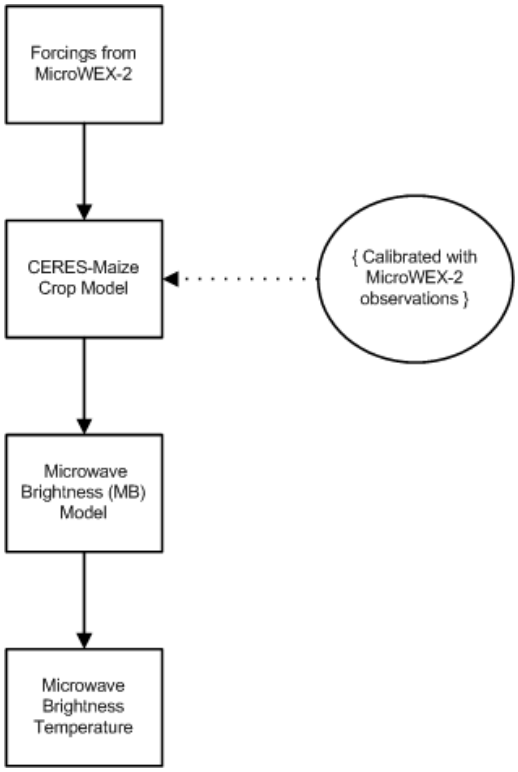

Figure 3. Flowchart of linkage of CERES-Maize model with the microwave brightness model.

Methodology

To calibrate the CERES-Maize model, a broad grid search was employed, followed by simulated annealing in the area of the global error minimum using the six cultivar coefficients. Each coefficient was incrementally changed, so that a grid of possible combinations of values, within the acceptable ranges, was tested to minimize the errors from biomass and LAI, the two most important canopy parameters required by the microwave brightness model. We excluded the LAI observation on DoY 135 for error minimization, due to its high standard deviation, as shown in figure 4c. The error (R) was computed as the sum of square errors, normalized by variance (Thornley and Johnson, 1990):

$$R = \frac{\mathrm{SSE}_B}{\sigma_B^2} + \frac{\mathrm{SSE}_{LAI}}{\sigma_{LAI}^2} \quad (7)$$

where SSE_B is the sum of square errors from total biomass, SSE_{LAI} is the sum of square errors from LAI, and σ^2_B and σ^2_{LAI} are the variances of biomass and LAI observations, respectively. The optimum combination of parameter values found by the grid search was then used as the initial guess in a simulated annealing optimization algorithm (Busetti, 2004). The RMSE, relative root mean square error (RRMSE), and Willmott d-index (Willmott, 1982) were calculated as for LAI and the biomass of each component, leaves, stems, and grain:

$$\mathrm{RMSE} = \sqrt{\frac{\sum (P_i - O_i)^2}{n}} \quad (8)$$

$$\mathrm{RRMSE} = \frac{\mathrm{RMSE}}{\overline{O}} \quad (9)$$

$$d = 1 - \frac{\sum (P_i - O_i)^2}{\sum (|P_i - \overline{P}| + |O_i - \overline{O}|)^2} \quad (10)$$

where n is the number of observations, P_i and O_i are the predicted and observed values, and $\overline{P}$ and $\overline{O}$ are the predicted and observed means. Table 1 shows the values of the six cultivar coefficients that minimized R in equation 7.

Linkage of CERES-Maize and Microwave Brightness Models

The model linkage is simple, as shown in figure 3. Soil moisture, soil temperature, air temperature, canopy biomass, and LAI from the CERES model are used by the microwave emission model (MB).

Results and Discussion

Crop Growth and Development

To evaluate the CERES-Maize model for crop growth and development, we compared model estimates of emergence and silking dates, biomass, and LAI to the observations during MicroWEX-2.

The modeled and observed emergence dates were on DoY 90 and DoY 86, respectively. Modeled anthesis day (when 75% of the corn has silked) was DoY 139, while we observed 75% silking by DoY 135. The model estimated realistic total dry biomass using the parameters determined by the grid search, as shown in figures 4a and 4b. The RMSE for biomass was 1.1 Mg/ha with a low RRMSE of 0.28 and a correspondingly high Willmott d-index of 0.98, as shown in . Figure 4b shows a scatter plot of estimated and observed total biomass. The biomass was increasingly underestimated by the model as the season progressed, with the maximum difference of 1.41 Mg/ha at the end of the season. The partitioning of the modeled biomass into leaf and stem biomass did not match the observations (fig. 4a), as indicated by the high RMSE and RRMSE in table 2. Partitioning of total biomass into stem biomass was underestimated by the model during later vegetative stages of growth (DoY 127 to DoY 134). The partitioning into leaf biomass was more realistic, with a slight overestimation during later growth stages (DoY 132 to DoY 142). The model's estimate of the beginning of grain fill at DoY 140 matched closely with the observed grain fill at DoY 139 (fig. 4a). The best fit for LAI and total biomass did not produce the best fit for grain fill. In order to compensate for the underestimated stem biomass, grain weight was overestimated. The model estimated realistic LAI, as seen in figures 4c and 4d, with a low RMSE and RRMSE of 0.10 and 0.074, respectively, and a high Willmott d-index of 0.99, as shown in table 2. Figure 4d shows the scatter plot of the model and observed LAI.

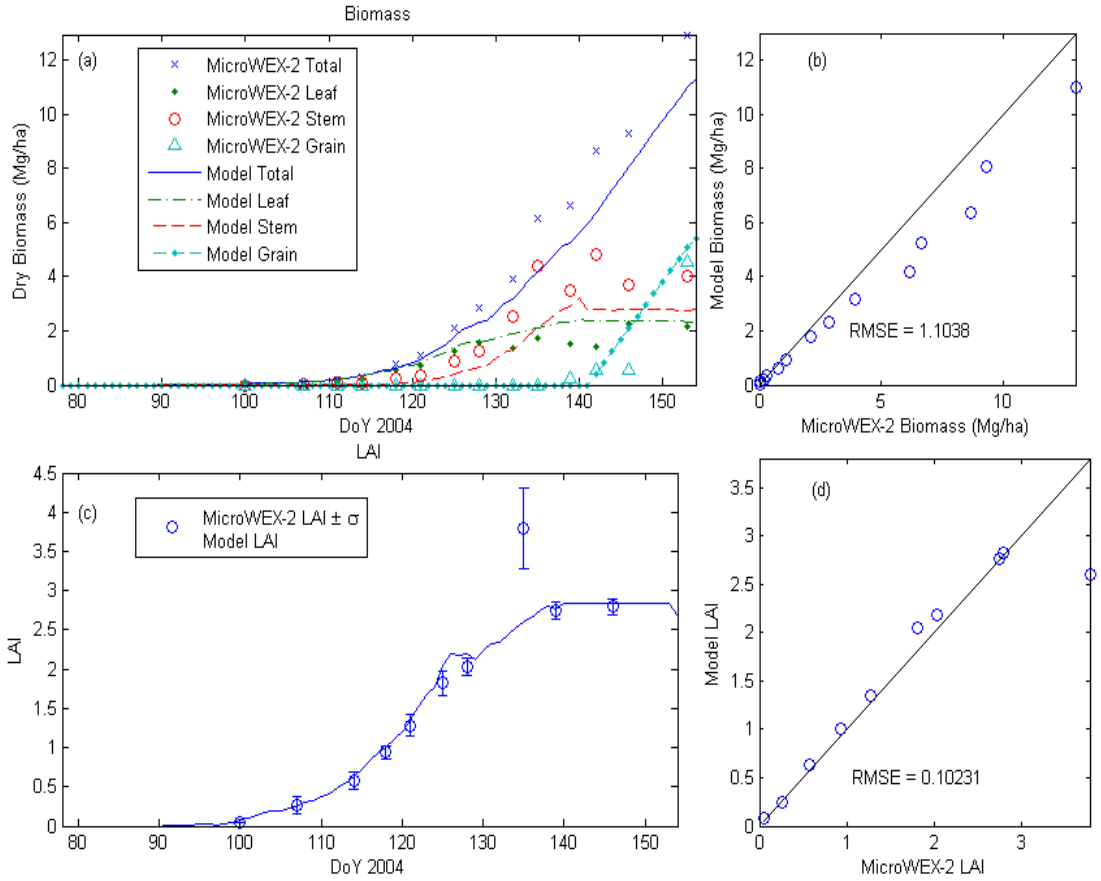

Figure 4. (a) Comparison of the CERES-Maize estimates and the observations of biomass during MicroWEX-2, (b) scatter plot of estimated and observed biomass, (c) comparison of the CERES-Maize estimates and the observations of LAI during MicroWEX-2, and (d) scatter plot of estimated and observed LAI.

Evapotranspiration

To understand model estimates of energy and moisture fluxes at the land surface, we compared the modeled daily latent heat flux with the observations during MicroWEX-2. We conducted four comparisons using two methods to estimate ET, RPT, and PFAO, and two values for the canopy light extinction coefficient (KCAN), 0.85 and 0.5 (Sau et al., 2004). Figure 5 shows a comparison of the latent heat flux estimates using the four methods. Even though the RMSE values were low (~40 W/m^2), the temporal distribution of latent heat fluxes was not estimated realistically during the growing season (fig. 5a). The latent heat fluxes were underestimated in the early season and overestimated (~100 W/m^2) during late season. The early season underestimation indicates low evaporation rates from the modeled soil, and the late season overestimation indicates higher transpiration rates in the modeled vegetation. The flux estimates were not as sensitive to KCAN values as the previous studies had found under water-stressed conditions (Sau et al., 2004). Daily under- or overestimations by the model effectively cancelled each other, so that the fit for cumulative ET was better than for the daily values (fig. 5b).

Table 2. Error statistics for crop growth and ET between CERES-Maize estimates and MicroWEX-2 field observations.

Parameter	RMSE	RRMSE	Willmott *d*
Total biomass (Mg/ha)	1.10	0.28	0.98
Stem biomass (Mg/ha)	1.02	0.55	0.89
Leaf biomass (Mg/ha)	0.39	0.37	0.94
Grain biomass (Mg/ha)	0.44	1.05	0.97
LAI	0.10	0.07	0.99
Latent heat flux (W/m^2)	42.07	0.39	0.87

Soil Moisture and Temperature

To understand the model performance regarding moisture and energy transport in soil, we compared modeled daily soil moisture and temperature profiles to the observed average daily values during MicroWEX-2 (figs. 6 and 7, table 3). We compared the average of observations at 2 and 4 cm to model estimates of 0-5 cm, average of 8 and 16 cm observations to the estimates of 5-15 cm, average of 16 and 32 cm observations to the estimates of 15-30 cm, observations at 32 cm to the estimates of 30-45 cm, average of 32 and 64 cm observations to the estimates of 45-60 cm, and average of 64 and 100 cm observations to the estimates of 60-90 cm.

The CERES-Maize model simulates moisture at daily timesteps, while the hydrological changes near the soil surface (0-5 cm) occur at much shorter timesteps, making it challenging to compare model and observed near-surface soil moisture. It is critical to understand the differences between the observed and modeled near-surface soil moisture because it strongly affects latent heat and sensible heat fluxes at the land surface and also affects microwave brightness signatures. Any significant errors in near-surface soil moisture estimates will result in unrealistic flux and brightness estimates. In figure 6a, we compare the daily moisture at

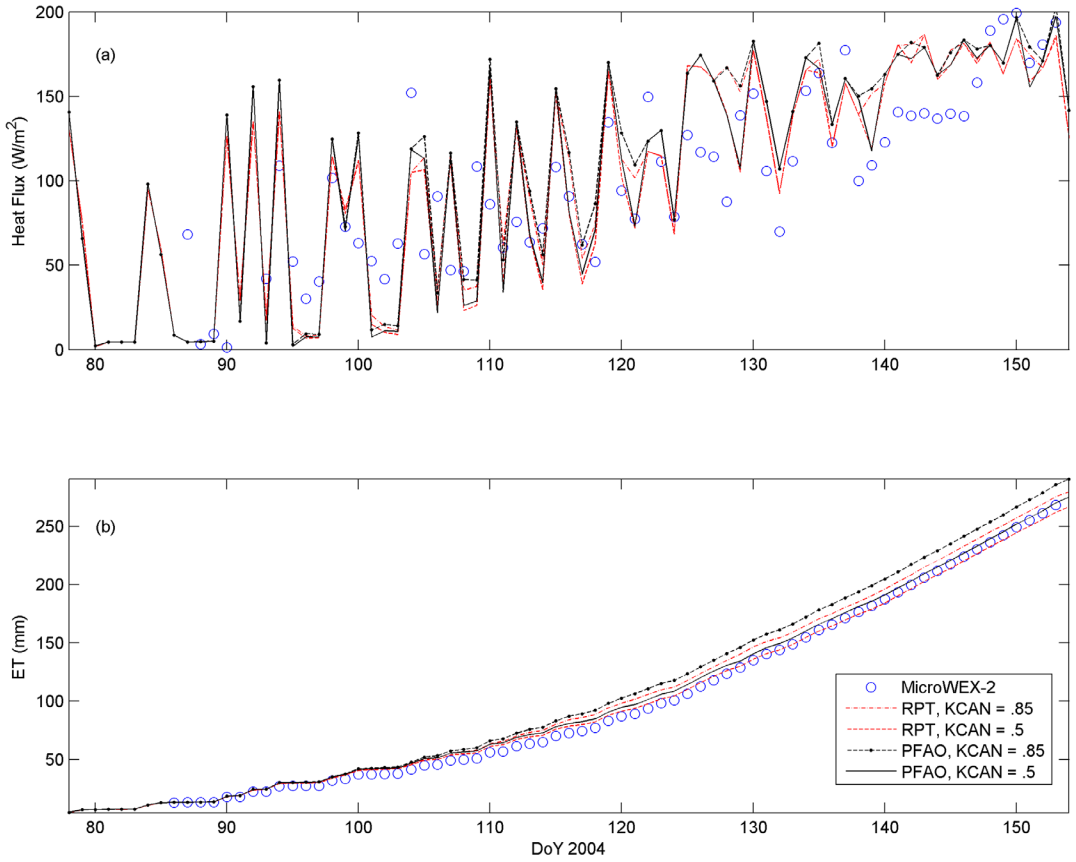

Figure 5. Comparison of the latent heat flux estimates from CERES-Maize model using four methods with the observations during MicroWEX-2 by (a) daily heat flux and (b) cumulative ET.

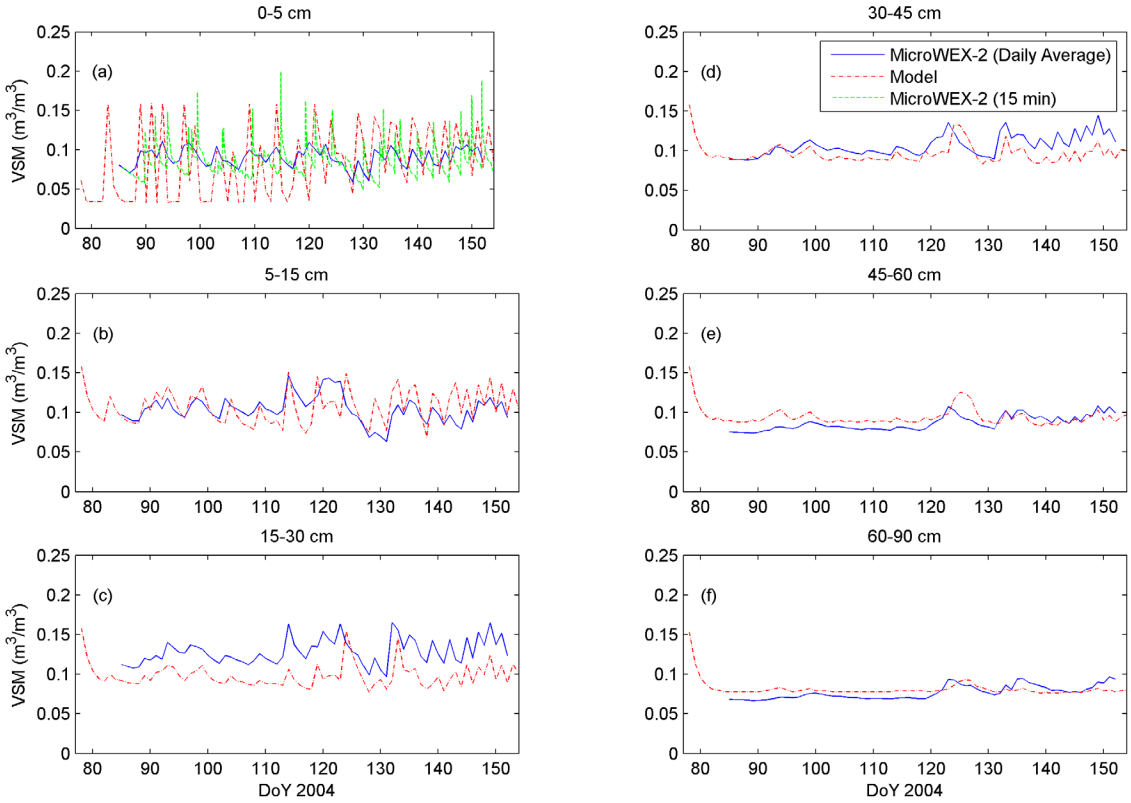

Figure 6. Comparison of the CERES-Maize volumetric soil moisture (VSM) estimates with MicroWEX-2 observations for: (a) 0-5 cm, (b) 5-15 cm, (c) 15-30 cm, (d) 30-45 cm, (e) 45-60 cm, and (f) 60-90 cm soil layers.

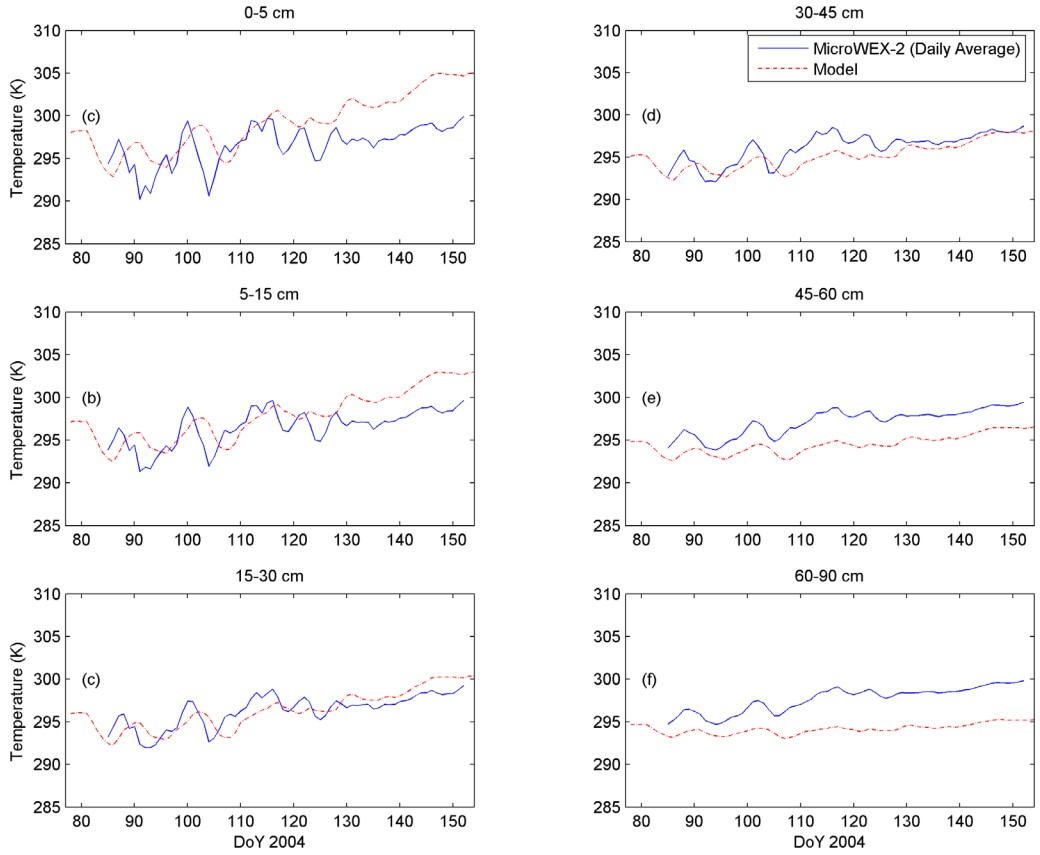

Figure 7. Comparison of the CERES-Maize soil temperature estimates with MicroWEX-2 observations for: (a) 0-5 cm, (b) 5-15 cm, (c) 15-30 cm, (d) 30-45 cm, (e) 45-60 cm, and (f) 60-90 cm soil layers.

0-5 cm estimated by the CERES-Maize model with daily averages and 15 min observations of volumetric soil moisture (VSM) during MicroWEX-2. Deeper soil layers matched the observed values fairly well, as suggested by their low RMSE values in table 3, except for a 3.4% underestimation during the entire growing season for the 15-30 cm layer. This error is within the experimental error of the observations made by the TDR probes.

Overall, the model did not capture the changes in soil temperatures realistically during the growing season. It estimated temperatures at depths of 15-45 cm fairly well, as indicated by their low RMSE values in table 3. The temperatures at deeper layers were underestimated throughout the growing season, with increasing differences as the season progressed. For the upper layers, the model did not capture the strong fluctuations in temperature closer to the surface. Significant errors in soil moisture and temperature profiles in the CERES-Maize model and the high sensitivity of flux and microwave brightness estimates to these parameters demonstrate a need for a more accurate method for determining energy and moisture transport in soil at shorter timesteps, with a higher vertical resolution in the top 5 cm of the soil.

Table 3. Error statistics for soil moisture and temperature between CERES-Maize estimates and MicroWEX-2 field observations.

	RMSE	
Soil Layer	Moisture (m^3/m^3)	Temperature (K)
5-15 cm	0.0204	2.534
15-30 cm	0.0344	1.426
30-45 cm	0.0164	1.485
45-60 cm	0.0117	2.775
60-90 cm	0.0083	3.648

Microwave Brightness

The MB model was used to simulate T_B by: (1) using only soil and vegetation data obtained during MicroWEX-2 and (2) using the soil and vegetation information when linked with the calibrated CERES-Maize model (crop-MB model). Figure 8 shows the horizontally polarized (H-pol) T_B estimated following the two methods during the growing season. Only H-pol T_B are discussed in this study because they are the most sensitive to changes in terrain moisture (Ulaby et al., 1981). The comparison allows us to examine the difference in brightness temperature estimates between inputs from observed field conditions and those from CERES-Maize, without the need for evaluating the MB model.

The overall seasonal trend is captured by both methods: using MicroWEX-2 inputs, and using CERES-Maize inputs (fig. 8). The RMS difference between the two H-pol microwave brightness outputs is 18.50 K. As the canopy biomass increases (fig. 4a), the contribution from soil is attenuated while the contribution from canopy emission is increased, raising H-pol brightness temperatures. However, the brightness estimated using the CERES inputs does not capture the diurnal variation in brightness because of its daily timestep. Because the microwave brightness signatures are sensitive to near-surface soil moisture changes, as seen from the time series plot of soil moisture (fig. 8), it is necessary to model brightness temperatures at shorter timesteps to capture these changes.

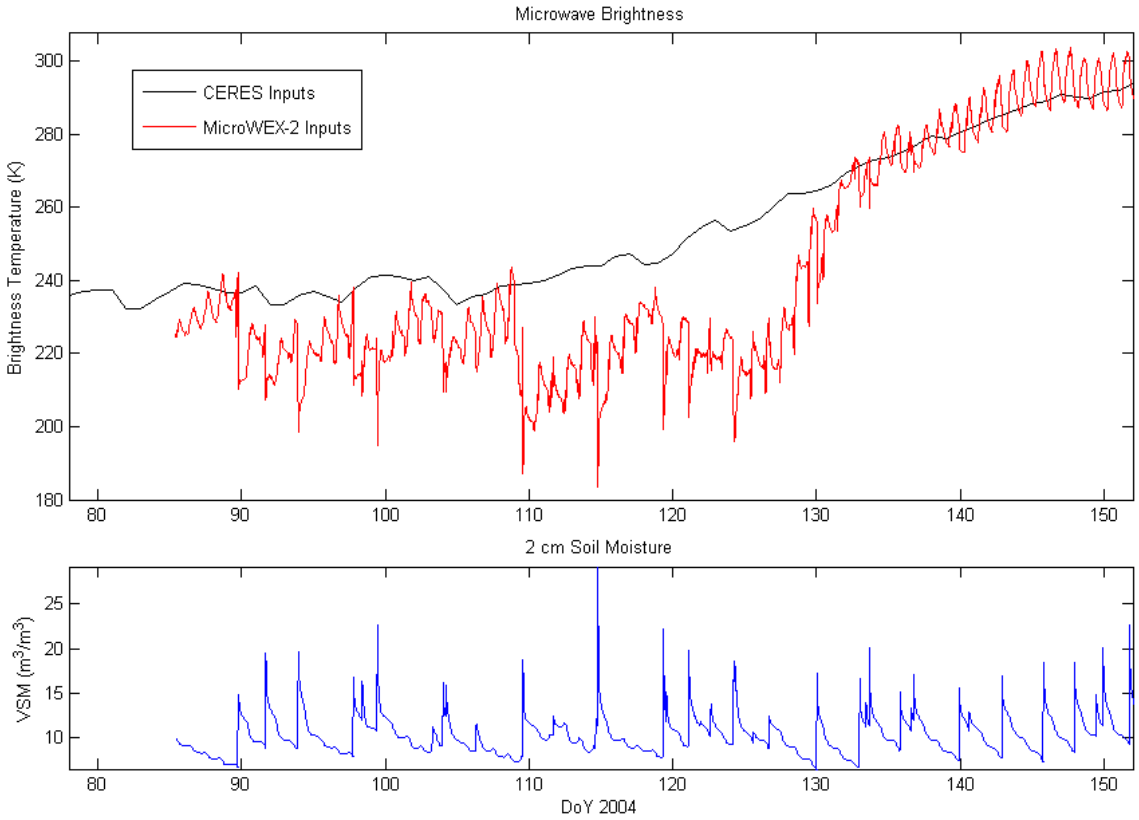

Figure 8. Modeled H-pol microwave brightness using (upper plots) measured MicroWEX-2 inputs and modeled CERES inputs and (lower plot) MicroWEX-2 surface soil moisture.

Conclusion

Crop growth models can be linked to microwave brightness models to utilize remotely sensed observations of brightness temperatures for improved estimates of ET, biomass, LAI, and yield. In this study, we developed a linked crop-MB model to estimate the brightness temperature for a growing corn canopy. CERES-Maize was calibrated using field observations from MicroWEX-2 during the corn growing season (DoY 78 to DoY 154) in 2004. The calibration was performed by minimizing errors for LAI and biomass, the two most important canopy parameters in determining the microwave signature of a vegetation canopy.

Overall, the CERES-Maize model estimated total biomass and LAI realistically. The partitioning of biomass into stem, leaf, and grain fill biomasses did not match well with the observations. The model underestimated biomass after midseason. The latent heat flux estimates were significantly overestimated in the early season and underestimated later in the season. The resulting fluxes were similar for both the RPT and PFAO methods and the two KCAN values. Soil moisture and temperature estimates, particularly near the surface, were not realistically modeled. The microwave brightness model was run with inputs from both CERES-Maize and from field observations; both ways showed the same seasonal trend, but CERES estimated higher brightness temperatures and failed to capture the diurnal variation of brightness temperatures. Because the energy fluxes and microwave brightness are highly sensitive to near-surface moisture and temperature distributions, and CERES cannot capture diurnal cycles in moisture and temperature, a more realistic energy and moisture transport module is suggested in the CERES-Maize model before it can be linked to an MB model.

Acknowledgements

This research was supported by the NSF Earth Science Directorate (EAR-0337277) and the NASA New Investigator Program (NASA-NIP-00050655). The authors would like to thank Mr. Orlando Lanni and Mr. Larry Miller for providing expert engineering support during MicroWEX-2; Mr. Jim Boyer and his team at the PSREU for land and crop management; and Mr. Kai-Jen Tien, Mr. Tzu-Yun Lin, and Ms. Mi-Young Jang for their help in data collection during MicroWEX-2. The authors would also like to acknowledge Dr. Gerritt Hoogenboom from the University of Georgia for his help in porting the DSSAT model to Linux OS and Dr. Ken Boote for assisting with development of the vegetation sampling protocol.

References

Attema, E., and F. Ulaby. 1978. Vegetation modeled as a water cloud. *Radio Science* 13(2): 357-364.

Bouman, B. A. M. 1992. Linking physical remote sensing models with crop growth simulation models, applied for sugar beet. *International J. Remote Sensing* 13(14): 2565-2581.

Brisson, N., B. Mary, D. Ripoche, M. H. Jeuffroy, F. Ruget, B. Nicoullaud, P.Gate, F. Devienne-Barret, R. Antonioletti, C. Durr, G. Richard, N. Beaudoin, S. Recous, X. Tayot, D. Plenet, P. Cellier, J. M. Machet, J. M. Meynard, and R. Delecolle . 1998. STICS: A generic model for the simulation of crops and their water and nitrogen balances: I. Theory and parameterization applied to wheat and corn. *Agronomie* 18(5-6): 311-346.

Burke, E., W. Shuttleworth, K. Lee, and L. Bastidas. 2001. Using area-average remotely sensed surface soil moisture in multipatch land data assimilation systems. *IEEE Trans. Geosci. Remote Sensing* 39(10): 2091-2100.

Busetti, F. 2004. Simulated annealing overview. Available at: www.geocities.com/francorbusetti/saweb.pdf.

Crow, W., and E. Wood. 2003. The assimilation of remotely sensed soil brightness temperature imagery into a land surface model using ensemble Kalman filtering: A case study based on ESTAR measurements during SGP97. *Adv. Water Resources* 26(2): 137-149.

Delécolle, R., S. J. Maas, M. Guerif, and F. Baret. 1992. Remote sensing and crop production models: Present trends. *ISPRS J. Photogramm. Remote Sensing* 47(2-3): 145-161.

Dobson, M. C., F. T. Ulaby, M. T. Hallikainen, and M. A. El-Rayes. 1985. Microwave dielectric behavior of wet soil part: II. Dielectric mixing models. *IEEE Trans. Geo. Remote Sensing* 23(1): 35-46.

Doorenbos, J., and W. Pruitt. 1977. Guidelines for predicting crop water requirements. Irrigation and drainage paper No. 24. Rome, Italy: United Nations FAO.

Doraiswamy, P., J. Hatfield, T. Jackson, B. Akhmedov, J. Prueger, and A. Stern. 2004. Crop condition and yield simulations using Landsat and MODIS. *Remote Sensing Environ.* 92(4): 548-559.

Du, Y., F. Ulaby, and M. Dobson. 2000. Sensitivity to soil moisture by active and passive microwave sensors. *IEEE Trans. Geosci. Remote Sensing* 38(1): 105-114.

Entekhabi, D., H. Nakamura, and E. Njoku. 1994. Solving the inverse problem for soil moisture and temperature profiles by sequential assimilation of multifrequency remotely sensed observations. *IEEE Trans. Geosci. Remote Sensing* 32(2): 438-448.

Galantowicz, J., D. Entekhabi, and E. Njoku. 2000. Estimation of soil-type heterogeneity effects in the retrieval of soil moisture from radio brightness. *IEEE Trans. Geosci. Remote Sensing* 3(1): 312-315.

Hoeben, R., and P. Troch. 2000. Assimilation of active microwave observation data for soil moisture profile estimation. *Water Resources Res.* 36(10): 2805-2819.

Houser, P., W. Shuttleworth, J. Famiglietti, H. Gupta, K. Syed, and D. Goodrich. 1998. Integration of soil moisture remote sensing and hydrologic modeling using data assimilation. *Water Resources Res.* 34(12): 3405-3420.

Jackson, T. 1993. Measuring surface soil moisture using passive microwave remote sensing. *Hydrological Processes* 7(22): 139-152.

Jackson, T., and P. O'Neill. 1987. Temporal observations of surface soil moisture using a passive microwave sensor. *Remote Sensing Environ.* 21(3): 281-296.

Jackson, T., D. LeVine, A. Hsu, A. Oldak, P. Starks, C. Swift, J. Ishman, and M. Haken. 1999. Soil moisture mapping at regional scales using microwave radiometry: The southern Great Plains hydrology experiment. *IEEE Trans. Geosci. Remote Sensing* 37(5): 2152-2158.

Jones, C., and J. Kiniry. 1986. CERES-Maize: A simulation model of maize growth and development. Tech. Report. College Station, Texas: Texas A&M University Press.

Jones, J., G. Hoogenboom, C. Porter, K. Boote, W. Batchelor, L. Hunt, P. Wilkens, U. Singh, A. Gijsman, and J. Ritchie. 2003. The DSSAT cropping system model. *European J. Agronomy* 18(3-4): 235-265.

Judge, J., J. J. Casanova, T. Lin, K. C. Tien, M. Jang, O. Lanni, and L. W. Miller. 2005. Field observations during the second microwave, water, and energy experiment (MicroWEX-2): from March 17 through June 3, 2004. Circular No. 1480. Gainesville, Fla.: University of Florida, Center for Remote Sensing. Available at: http://edis.ifas.ufl.edu/AE360.

Lakshmi, V. 2000. A simple surface temperature assimilation scheme for use in land surface models. *Water Resources Res.* 36(12): 3687-3700.

Maas, S. J., R. D. Jackson, S. B. Idso, P. J. Pinter, Jr., and R. J. Reginato. 1989. Incorporation of remotely sensed indicators of water stress in a crop growth simulation model. In *Proc. 19th Conference on Agriculture and Forest Meteorology*, 228-231. Washington, D.C.: American Meteorological Society.

Manabe, S. 1969. Climate and the ocean circulation: 1. The atmosphere circulation and the hydrology of the earth's surface. *Monthly Weather Rev.* 97(11): 739-774.

Moulin, S., A. Bondeau, and R. Delecolle. 1998. Combining agricultural crop models and satellite observations from field to regional scales. *Int. J. Remote Sensing* 19(6): 1021-1036.

Prevot, L., H. Chauki, D. Troueau, M. Weiss, F. Baret, and N. Brisson. 2003. Assimilating optical and radar data into the STICS crop model for wheat. *Agronomie* 23(4): 297-303.

Reichle, R., D. McLaughlin, and D. Entekhabi. 2002. Hydrologic data assimilation with the ensemble Kalman filter. *Monthly Weather Rev.* 130(1): 103-114.

Ritchie, J. 1972. Model for predicting evaporation from a row crop with incomplete cover. *Water Resources Res.* 8(5): 1204-1213.

Sau, F., K. Boote, W. M. Bostick, J. Jones, and M. I. Minguez. 2004. Testing and improving evapotranspiration and soil water balance of the DSSAT crop models. *Agronomy J.* 96(5): 1243-1257.

Schmugge, T., and T. Jackson. 1991. A dielectric model of the vegetation effects on the microwave emission of moist soils. *IEEE Trans. Geosci. Remote Sensing* 30(4) 757-759.

Thornley, J., and I. Johnson. 1990. *Plant and Crop Modeling.* U.K.: Oxford University Press.

Ulaby, F. Y., R. K. Moore, and A. K. Fung. 1981. *Microwave Remote Sensing: Active and Passive.* Norwood, Mass.: Artech House.

USDA-ARS. 2004. SMEX04. Available at: http://hydrolab.arsusda.gov/smex04/.

USDA-SCS. 1972. Section 4: Hydrology. In *National Engineering Handbook.* Washington D.C.: USDA-SCS.

Van Leeuwen, H. J. C., and J. G. P. W. Clevers. 1994. Synergy between optical and microwave remote sensing for crop monitoring. In *6th Symp. ISPRS: Physical Measurements and Signatures in Remote Sensing*, 1175-1182. International Society for Photogrammetry and Remote Sensing.

Walker, J., and P. Houser. 2001. A methodology for initializing soil moisture in a global climate model: Assimilation of near-surface soil moisture observations. *J. Geophys. Res.* 106(D11): 11761-11774.

Williams, J. R., C. A. Jones, J. R. Kiniry, and D. A. Spanel. 1989. The EPIC crop growth model. *Trans. ASAE* 32(2): 497-511.

Willmott, C. J. 1982. Some comments on the evaluation of model performance. *Bulletin of the American Meteorological Society* 63(11): 1309-1313.